Centrality Dependence of the Charged Particle Multiplicity near Mid-Rapidity in Au+Au Collisions at $\sqrt{s_{NN}} = 130$ and 200 GeV

B.B.Back[1], M.D.Baker[2], D.S.Barton[2], R.R.Betts[6], R.Bindel[7], A.Budzanowski[3], W.Busza[4], A.Carroll[2], J.Corbo[2], M.P.Decowski[4], E.Garcia[6], N.George[1], K.Gulbrandsen[4], S.Gushue[2], C.Halliwell[6], J.Hamblen[8], C.Henderson[4], D.Hicks[2], D.Hofman[6], R.S.Hollis[6], R.Hołyński[3], B.Holzman[2], A.Iordanova[6], E.Johnson[8], J.Kane[4], J.Katzy[4,6], N.Khan[8], W.Kucewicz[6], P.Kulinich[4], C.M.Kuo[5], W.T.Lin[5], S.Manly[8], D.McLeod[6], J.Michałowski[3], A.Mignerey[7], J.Mülmenstädt[4], R.Nouicer[6], A.Olszewski[3], R.Pak[2], I.C.Park[8], H.Pernegger[4], M.Rafelski[2], M.Rbeiz[4], C.Reed[4], L.P.Remsberg[2], M.Reuter[6], C.Roland[4], G.Roland[4], L.Rosenberg[4], J. Sagerer[6], P.Sarin[4], P.Sawicki[3], W.Skulski[8], S.G.Steadman[4], P.Steinberg[2], G.S.F.Stephans[4], M.Stodulski[3], A.Sukhanov[2], J.-L.Tang[5], R.Teng[8], A.Trzupek[3], C.Vale[4], G.J.van Nieuwenhuizen[4], R.Verdier[4], B.Wadsworth[4], F.L.H.Wolfs[8], B.Wosiek[3], K.Woźniak[2,3], A.H.Wuosmaa[1], B.Wysłouch[4]

(PHOBOS Collaboration)

[1] Physics Division, Argonne National Laboratory, Argonne, IL 60439-4843

[2] Chemistry and C-A Departments, Brookhaven National Laboratory, Upton, NY 11973-5000

[3] Institute of Nuclear Physics, Kraków, Poland

[4] Laboratory for Nuclear Science, Massachusetts Institute of Technology, Cambridge, MA 02139-4307

[5] Department of Physics, National Central University, Chung-Li, Taiwan

[6] Department of Physics, University of Illinois at Chicago, Chicago, IL 60607-7059

[7] Department of Chemistry, University of Maryland, College Park, MD 20742

[8] Department of Physics and Astronomy, University of Rochester, Rochester, NY 14627

(January 3, 2002)

The PHOBOS experiment has measured the charged particle multiplicity at mid-rapidity in Au+Au collisions at $\sqrt{s_{NN}} = 200$ GeV as a function of the collision centrality. Results on $dN_{ch}/d\eta|_{|\eta|<1}$ divided by the number of participating nucleon pairs $\langle N_{part}\rangle/2$ are presented as a function of $\langle N_{part}\rangle$. As was found from similar data at $\sqrt{s_{NN}} = 130$ GeV, the data can be equally well described by parton saturation models and two-component fits which include contributions that scale as N_{part} and the number of binary collisions N_{coll}. We compare the data at the two energies by means of the ratio $R_{200/130}$ of the charged particle multiplicity for the two different energies as a function of $\langle N_{part}\rangle$. For events with $\langle N_{part}\rangle > 100$, we find that this ratio is consistent with a constant value of $1.14 \pm 0.01(stat.) \pm 0.05(syst.)$.

Collisions of gold nuclei at the Relativistic Heavy-Ion Collider (RHIC) at $\sqrt{s_{NN}} = 200$ GeV offer a means to study strongly-interacting matter at high densities and temperatures. The goal is to create a large-volume, long-lived state within which quarks and gluons are no longer confined within hadrons, the quark-gluon plasma (QGP). The role of the collision geometry in determining the initial parton configuration is important for understanding any collective effects which may be present in such collisions. We can study this by means of the mid-rapidity charged particle multiplicity as a function of the number of nucleons that participate in the collision, N_{part}. Measurements of proton-nucleus reactions at lower energies [1] suggested that the charged multiplicity from soft production mechanisms should simply scale with N_{part} [2]. With increasing energy, however, one might expect some component of particle production to depend on the number of binary collisions, due to the increasing role of hard processes (minijet and jet production). In nuclear collisions, $\langle N_{coll}\rangle \propto \langle N_{part}\rangle^{4/3}$, making these systems quite suitable for studying the interplay between the various effects.

Nuclear collisions at RHIC also provide an opportunity to study Quantum Chromodynamics (QCD) in a novel regime where parton densities are high, yet the strong coupling constant is small due to the large momentum transfers involved. In such a regime, gluon densities can be large enough that the gluons recombine, causing a saturation of the gluon structure function at low Bjorken x, characterized by a momentum scale Q_s. Since the parton densities in the initial state can be related to the density of produced hadrons in the final state, definite predictions are possible regarding the multiplicity of charged particles as a function of energy and centrality [3].

A recent extension of the calculations by Kharzeev and Levin [4] has given predictions of the energy, rapidity, and centrality dependence of the charged particle multiplicity. These new calculations use the predicted QCD evolution of measured results, incorporating parameters extracted from inclusive deep-inelastic electron-proton scattering data [5]. Of primary importance in this treatment is the exponent λ, which parameterizes the energy dependence of the saturation scale as $Q_s^2 \propto (\sqrt{s})^\lambda$. Kharzeev and Levin use this to predict that the energy dependence for $dN_{ch}/d\eta$ will also scale as $(\sqrt{s})^\lambda$ at high energies. Furthermore, they predict that the higher energy collisions allow events with larger impact parameter to be in the saturation regime. This affects the multiplicity from peripheral events more than for central events, which already have sufficient parton density at lower energies. Thus, they predict the multiplicity in peripheral events to rise slightly faster with energy than for central events.

This effect should be contrasted with the much simpler two-component parameterization constructed to interpolate between proton-(anti)proton ($pp, \overline{p}p$) and central nucleus-nucleus collisions by incorporating contributions which scale with the number of wounded nucleons as well as the number of binary collisions. The pseudorapidity density at mid-rapidity has been measured to rise by 14±5% between 130 and 200 GeV in central $Au+Au$ collisions [6] while interpolations based on UA5 data on $\overline{p}p$ collisions at similar energies [7] suggest only an 8% increase for elementary collisions. Therefore, the ratio $R_{200/130} = dN_{ch}/d\eta|_{200}/dN_{ch}/d\eta|_{130}$ should decrease with increasing impact parameter.

The predictions from the saturation and two-component scenarios have been found to be nearly indistinguishable as a function of centrality at $\sqrt{s_{NN}} = 130$ GeV [3,8] and agree well with the published RHIC data from PHENIX [9] and PHOBOS [10,11]. The authors of Ref. [8] find this to be a nontrivial consequence of the saturation formalism, although this ambiguity is unlikely to be reduced on the basis of the multiplicity data alone.

We have performed a measurement of the centrality dependence of the mid-rapidity charged particle multiplicity in Au+Au collisions at $\sqrt{s_{NN}} = 200$ GeV using the PHOBOS detector and derived $R_{200/130}$ as a function of the number of participants. PHOBOS has previously published results for the centrality dependence of $dN_{ch}/d\eta/(\frac{1}{2}\langle N_{part}\rangle)$ at $\sqrt{s_{NN}} = 130$ GeV [10] as well as $R_{200/130}$ for the 6% most central events ($\langle N_{part}\rangle \sim 343$) [6]. The present results are an extension to the previous measurements, using similar methods of analysis.

The collision centrality is determined using the signals measured in two sets of 16 paddle counters (PP and PN) located at $|z| = 3.21$ m with respect to the nominal interaction point. For events at $z = 0$, these detectors measure charged particles produced into $3 < |\eta| < 4.5$. As discussed in Ref. [10], we rely on the monotonicity of the paddle signal with the number of participants (verified by correlations with the PHOBOS zero-degree calorimeters) to extract $\langle N_{part}\rangle$ for a chosen fraction of the total cross section, based on the Glauber calculation used by the HIJING model [12]. The dominant systematic error on this quantity reflects the uncertainty on the estimation of the total cross section observed by the PHOBOS trigger counters. By a study of events with a low number of hit paddles using a full simulation of HIJING events, we have estimated the efficiency for triggering on the Au+Au total inelastic cross section to be $96 \pm 3\%$ for $\sqrt{s_{NN}} = 130$ GeV and $97 \pm 3\%$ for $\sqrt{s_{NN}} = 200$ GeV. The slight difference between the two energies stems mainly from the increase in the width of the pseudorapidity distribution [6]. In order to reduce the error on the ratio of the multiplicity as a function of centrality, we have analyzed the simulations at both energies in an identical fashion. This has led to a slightly different efficiency at $\sqrt{s_{NN}} = 130$ GeV than the one presented in Ref. [10], which was $97 \pm 3\%$.

The charged particle multiplicity has been measured independently for each energy using the same technique described in [10], based on counting 3-point tracks ("tracklets") in the spectrometer and vertex detectors. This approach permits some level of background rejection relative to simply counting detector hits, as was done in [11]. We use a simulation based on HIJING events and a full GEANT simulation to study the effects of occupancy, combinatorial background and experimental backgrounds. Due to the better granularity in both pseudorapidity and azimuthal angle in the spectrometer, its associated systematic error is 4.5%, to be compared with 7.5% in the vertex detector. As the particle density does not increase dramatically between the two energies, the systematic error is the same for the two data sets.

In forming the ratio $R_{200/130}$, we have analyzed the data in each subdetector with the same correction factors for both energies. This reduces the importance of the precision of the Monte Carlo simulations used to derive the corrections at each energy, since they directly cancel in the final value of $R_{200/130}$. This is justified by the fact that the particle density does not change substantially between the two energies.

We present two forms of $R_{200/130}$. The first is done for a chosen fraction of the total cross section, which requires no other input other than the trigger efficiency. The other is the ratio for a constant value of N_{part}, which requires a model of the nuclear geometry. In both cases, a precise measurement of the $R_{200/130}$ is achieved by the average of separate measurements of the ratio in each sub-detector.

In Fig.1(a) we show the ratio of $dN_{ch}/d\eta|_{|\eta|<1}$ at $\sqrt{s_{NN}} = 130$ GeV and 200 GeV for the same percentile of the total cross section, $R^{raw}_{200/130}$. The values in each bin are listed in the last column of Table I. This is found to be approximately constant for the 50% most central collisions. The grey band indicates the magnitude of the systematic error, which is symmetric around the shown data points. It reflects the uncertainty in the estimate of the relative uncertainty of the trigger efficiency between the two center-of-mass energies.

The ratio of the charged particle multiplicity between $\sqrt{s_{NN}} = 200$ and 130 GeV as a function of the number of participants has been obtained simply by taking the ratio of $dN_{ch}/d\eta|_{|\eta|<1}/(\frac{1}{2}\langle N_{part}\rangle)$ for the two energies, which corrects for the increase of the inelastic cross section between $\sqrt{s_{NN}}$ = 130 and 200 GeV (as parameterized in HIJING). The increasing cross section causes the ratio of $\langle N_{part}\rangle$ between the two energies in each centrality bin, $N^{200}_{part}/N^{130}_{part}$, to increase by approximately 3% between the most central events and the bin corresponding to 45-50% of the total cross section ($\langle N_{part}\rangle = 65$), as shown in Fig. 1(b).

It should be emphasized that in both ratio measurements, averaging over independently-measured ratios does not give precisely the same answer as that of taking the ratios of the averaged quantity at each beam energy. We have chosen the former method since it allows the correction factors for each measurement to cancel in the ratio.

In Fig. 2(a) we present the separate results for $dN_{ch}/d\eta/(\frac{1}{2}\langle N_{part}\rangle)$ vs. N_{part} for $\sqrt{s_{NN}}$ = 200 GeV (shown as closed triangles) as well as 130 GeV (open triangles). For both energies, we observe a continuous rise of particle density with increasing centrality. The total 95% C.L. error for the 200 GeV data is shown as a shaded band and includes both statistical and systematic errors. The errors at 130 GeV are not shown, but are of similar magnitude. In Table I, we list $\langle N_{part}\rangle$, $dN_{ch}/d\eta|_{|\eta|<1}$ and $dN_{ch}/d\eta|_{|\eta|<1}/(\frac{1}{2}\langle N_{part}\rangle)$ for each energy and centrality bin.

To put these results in context, we also show two calculations. The first calculation shown is the prediction of the parton saturation model for both energies, indicated by solid lines in Fig. 2(a). The only parameter needed to predict the energy density is the exponent λ, which is set to 0.25 as is done in Ref. [4]. The calculation is truncated at $\langle N_{part}\rangle \sim 65$ since this model is not appropriate below this value [3].

The second calculation involves fits to the data using the two-component parameterization proposed in Ref. [3], $dN_{ch}/d\eta = n_{pp}((1-x)\langle N_{part}\rangle/2 + x\langle N_{coll}\rangle)$. The parameters have a simple interpretation as the fraction of production from hard processes (x) and the number of particles associated with a single pp interaction (n_{pp}) when N_{part} = 2 and N_{coll} = 1. We have performed fits using a parameterization of $\langle N_{coll}\rangle$ based on Ref. [3], $\langle N_{coll}\rangle = 0.352 \times \langle N_{part}\rangle^{1.37}$. Using the measured values for n_{pp} we find that values of $x = 0.09 \pm 0.02$ for $\sqrt{s_{NN}}$ = 130 GeV and $x = 0.11 \pm 0.02$ for $\sqrt{s_{NN}}$ = 200 GeV account well for the measured centrality dependence of $dN_{ch}/d\eta/(\frac{1}{2}\langle N_{part}\rangle)$. These are shown as dashed lines in Fig. 2(a). The error estimate is based on the allowed range of x which keeps the results of the calculation within our stated error bands. The value of x obtained for $\sqrt{s_{NN}}$ = 130 GeV agrees with the value extracted in Ref. [3], which only used the $\overline{p}p$ value and the central PHOBOS result from Ref. [13]. The value of x at $\sqrt{s_{NN}}$ = 200 GeV is consistent with the prediction in Ref. [4] that x should vary as the square of the minijet cross section, $(\sqrt{s_{NN}})^{2\lambda}$, which gives $x(\sqrt{s_{NN}} = 200) = 1.2 \times x(\sqrt{s_{NN}} = 130)$ for $\lambda = .25$. These results are also in good agreement with the two-component calculations by Li and Wang [14], which use recent parameterizations of the gluon structure functions as well as nuclear shadowing.

The centrality dependence of $R_{200/130}$ is shown in Fig. 2(b) and shown in Table I. The error bars indicate the contribution from counting statistics, which becomes important when the systematic effects cancel. The systematic error on the centrality dependence of the ratio, whose magnitude is shown by the grey band, is symmetric around the shown data points and incorporates two major contributions. The first is the uncertainty in the relative trigger efficiency between the two energies, which is shown in Fig. 1(a). The second error source is the change in N_{part} for a given centrality bin as a function of energy, shown in Fig. 1(b). We have added half of this difference in quadrature with the first contribution to get the final systematic error. In addition, there is an overall scale uncertainty on $R_{200/130}$ and $R^{raw}_{200/130}$ of 5%, which was discussed in Ref. [6] and stems from the Monte Carlo studies from which we derived our acceptance, feed-down, and background corrections. If we fit the ratio vs. N_{part} to a constant $R_{200/130}$ above $\langle N_{part}\rangle = 100$, we find that it is equal to $1.14 \pm 0.01(stat)$.

For N_{part} = 2 we show the ratio of data from $\overline{p}p$ for $\sqrt{s_{NN}}$ = 200 GeV and an interpolation for $\sqrt{s_{NN}}$ = 130 GeV [7]. We also show the ratios of the saturation model predictions (solid line) and the two-component fits (dashed line) from Fig. 2(a). While the two calculations evolve in opposite directions as the impact parameter increases, they remain sufficiently close down to $\langle N_{part}\rangle \sim 65$ such that our present data cannot resolve them definitively.

In conclusion, the PHOBOS collaboration has measured the pseudorapidity density of charged particles produced at mid-rapidity in Au+Au collisions at $\sqrt{s_{NN}}$ = 200 GeV. These data have been compared to similar data taken at $\sqrt{s_{NN}}$ = 130 GeV by taking the ratio of multiplicities $R_{200/130}$ at a fixed value of $\langle N_{part}\rangle$. For $\langle N_{part}\rangle > 100$, we find that this ratio is approximately constant at $1.14 \pm 0.01(stat.) \pm 0.05(syst.)$, which is consistent both with the parton saturation model predictions and two-component fits to the data.

This work was partially supported by US DoE grants DE-AC02-98CH10886, DE-FG02-93ER40802, DE-FC02-94ER40818, DE-FG02-94ER40865, DE-FG02-99ER41099, W-31-109-ENG-38 and NSF grants 9603486, 9722606 and 0072204. The Polish groups were partially supported by KBN grant 2 P03B 04916. The NCU group was partially supported by NSC of Taiwan under contract NSC 89-2112-M-008-024. We would especially like to thank D. Kharzeev and X.-N. Wang for helpful

discussions.

[1] J. E. Elias, *et al.*, Phys. Rev. D **22**, 13 (1980).
[2] A. Białas, B. Bleszyński and W. Czyż, Nucl. Phys. **B111** 461 (1976).
[3] D. Kharzeev and M. Nardi, Phys. Lett. B **507**, 121 (2001).
[4] D. Kharzeev and E. Levin, arXiv:nucl-th/0108006.
[5] K. Golec-Biernat and M. Wusthoff, Phys. Rev. D **60**, 114023 (1999).
[6] B. B. Back *et al.*, arXiv:nucl-ex/0108009, accepted to Phys. Rev. Lett.
[7] F. Abe *et al.*, Phys. Rev. **D41** 2330 (1990).
[8] J. Schaffner-Bielich, D. Kharzeev, L. D. McLerran and R. Venugopalan, nucl-th/0108048.
[9] K. Adcox *et al.*, Phys. Rev. Lett. **86**, 3500 (2001).
[10] B. B. Back *et al.*, arXiv:nucl-ex/0105011, accepted to Phys. Rev. C - Rapid Communications.
[11] B. B. Back *et al.*, Phys. Rev. Lett. **87**, 102303 (2001).
[12] M. Gyulassy and X.-N. Wang, Phys. Rev. **D44** 3501 (1991).
[13] B. B. Back *et al.*, Phys. Rev. Lett. **85**, 3100 (2000).
[14] S. y. Li and X. N. Wang, arXiv:nucl-th/0110075.

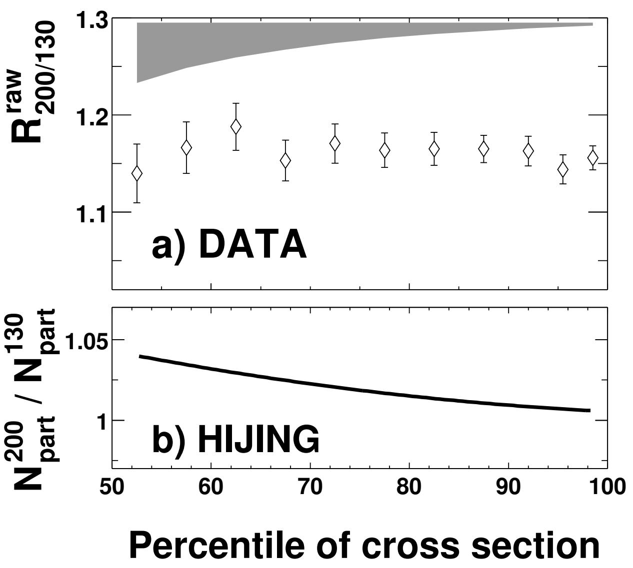

FIG. 1. a.) $R^{raw}_{200/130}$ vs. the average percentile of cross section. The grey band indicates the systematic error induced by the uncertainty in the relative trigger efficiency between the two beam energies. b.) The ratio $N^{200}_{part}/N^{130}_{part}$ for each centrality bin derived using HIJING at $\sqrt{s_{NN}} = 130$ and 200 GeV.

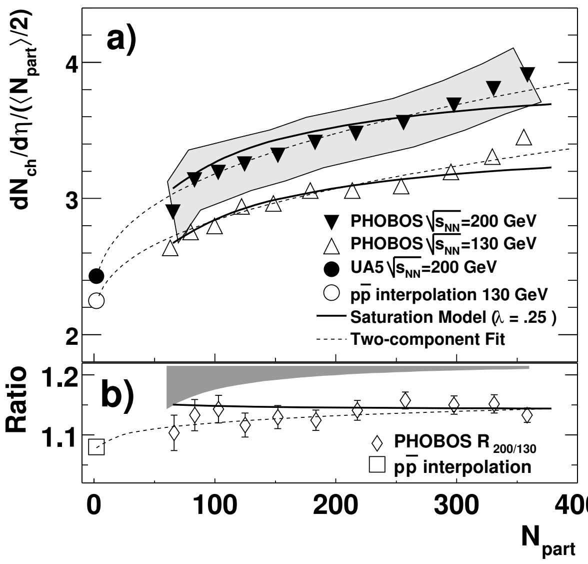

FIG. 2. a.) The measured scaled pseudorapidity density $dN_{ch}/d\eta|_{|\eta|<1}/(\frac{1}{2}\langle N_{part}\rangle)$ as a function of N_{part} for Au+Au collisions at $\sqrt{s_{NN}} = 130$ GeV (open triangles) and 200 GeV (closed triangles). The error band around the 200 GeV data combines the error on $dN_{ch}/d\eta|_{|\eta|<1}$ and $\langle N_{part}\rangle$. The open and solid circles are $\overline{p}p$ results derived from the data in Ref. [7]. b.) The ratio of charged multiplicity for $\sqrt{s_{NN}} = 130$ and 200 GeV, $R_{200/130}$, (for constant $\langle N_{part}\rangle$) vs. N_{part}. The ratio from $\overline{p}p$ is shown by the open square. The grey band indicates the systematic error estimate. In both panels, results from a saturation model prediction and a two-component fit are shown as solid and dashed lines, respectively.

TABLE I. For each centrality bin, based on the percentile of the total cross section, we show the pseudorapidity density, the number of participants, and the scaled pseudorapidity density for both $\sqrt{s_{NN}} = 130$ and 200 GeV. We also show the ratio $R_{200/130}$ for each bin both corrected for the different N_{part} in each bin, and uncorrected ("raw"). Errors are statistical only.

	200 GeV			130 GeV			Ratios	
Bin(%)	$dN_{ch}/d\eta$	$\langle N_{part}\rangle$	$dN_{ch}/d\eta/(\frac{1}{2}\langle N_{part}\rangle)$	$dN_{ch}/d\eta$	$\langle N_{part}\rangle$	$dN_{ch}/d\eta/(\frac{1}{2}\langle N_{part}\rangle)$	$R_{200/130}$	$R^{raw}_{200/130}$
0 - 3	700 ± 27	358 ± 12	3.91 ± 0.20	613 ± 24	355 ± 12	3.45 ± 0.17	1.13 ± 0.01	1.16 ± 0.01
3 - 6	629 ± 24	331 ± 10	3.81 ± 0.18	545 ± 21	330 ± 10	3.31 ± 0.16	1.15 ± 0.02	1.14 ± 0.02
6 - 10	548 ± 21	298 ± 9	3.68 ± 0.18	472 ± 18	295 ± 9	3.20 ± 0.16	1.15 ± 0.02	1.16 ± 0.02
10 - 15	455 ± 18	256 ± 8	3.56 ± 0.18	393 ± 15	254 ± 8	3.09 ± 0.16	1.16 ± 0.01	1.16 ± 0.01
15 - 20	376 ± 15	217 ± 8	3.48 ± 0.18	327 ± 13	214 ± 8	3.06 ± 0.16	1.14 ± 0.02	1.17 ± 0.02
20 - 25	312 ± 12	183 ± 7	3.41 ± 0.18	274 ± 11	179 ± 7	3.06 ± 0.17	1.12 ± 0.02	1.16 ± 0.02
25 - 30	252 ± 10	152 ± 6	3.32 ± 0.19	220 ± 8	148 ± 6	2.96 ± 0.17	1.13 ± 0.02	1.17 ± 0.02
30 - 35	202 ± 8	124 ± 6	3.25 ± 0.19	180 ± 7	122 ± 6	2.94 ± 0.18	1.12 ± 0.02	1.15 ± 0.02
35 - 40	164 ± 6	103 ± 5	3.19 ± 0.21	140 ± 5	100 ± 5	2.80 ± 0.18	1.14 ± 0.02	1.19 ± 0.02
40 - 45	130 ± 5	83 ± 5	3.14 ± 0.22	110 ± 4	80 ± 5	2.75 ± 0.20	1.13 ± 0.03	1.17 ± 0.03
45 - 50	95 ± 4	65 ± 4	2.90 ± 0.22	83 ± 3	63 ± 4	2.64 ± 0.21	1.10 ± 0.03	1.14 ± 0.03